

Effect of neutron and γ -ray on charge-coupled device for vacuum/extreme ultraviolet spectroscopy in deuterium discharges of Large Helical Device ^{a)}

Y. Liu^{1,b)}, S. Morita^{1,2}, T. Oishi^{1,2} and M. Goto^{1,2}

¹*Department of Fusion Science, Graduate University for Advanced Studies, Toki 509-5292, Gifu, Japan*

²*National Institute for Fusion Science, Toki 509-5292, Gifu, Japan*

(Presented XXXXX; received XXXXX; accepted XXXXX; published online XXXXX)

(Dates appearing here are provided by the Editorial Office)

Charge-coupled device (CCD) is widely used as a detector of vacuum spectrometers in fusion devices. Recently, a deuterium plasma experiment has been initiated in Large Helical Device (LHD). Totally 3.7×10^{18} neutrons have been yielded with energies of 2.45 MeV (D-D) and 14.1 MeV (D-T) during the deuterium experiment over four months. Meanwhile, γ -rays are radiated from plasma facing components and laboratory structural materials in a wide energy range, i.e., 0.01-12.0 MeV, through the neutron capture. It is well known that these neutrons and γ -rays bring serious problems to the CCD system. Then, several CCDs of vacuum ultraviolet (VUV) / extreme ultraviolet (EUV) / X-ray spectrometers installed at different locations on LHD for measurements of spectra and spatial profiles of impurity emission lines are examined to study the effect of neutrons and γ -rays. An additional CCD placed in a special shielding box made of 10 cm thick polyethylene contained 10% boron and 1.5 cm thick lead is also used for the detailed analysis. As a result, it is found that the CCD has no damage in the present neutron yield of LHD, while the background noise integrated for all pixels of CCD largely increases, i.e., $1-3 \times 10^8$ counts/s. The data analysis of CCD in the shielding box shows that the background noise caused by the γ -ray is smaller than that caused by the neutron, i.e., 41% from γ -rays and 59% from neutrons. It is also found that the noise can be partly removed by an accumulation of CCD frames or software programming.

I. INTRODUCTION

In fusion research, charge-coupled device (CCD) has been commonly used for spectroscopic diagnostic systems.¹⁻⁹ Since deuterium (D) gas is usually used for fueling in the fusion experiment to maintain the discharge, a lot of neutrons with energy of 2.45 MeV are produced during the D-D operation. Tritons (T) generated by the D-D reaction have a subsequent reaction with the deuteron, i.e., D-T reaction, and yield a neutron with higher energy of 14.1 MeV. It is well known such neutrons cause serious problems to the CCD system, including a background noise. In addition, γ -rays produced through the neutron capture are emitted from plasma facing components and laboratory structural materials, which also create a huge background noise on the CCD.¹⁰⁻¹² These noises lower the CCD capability of measuring a high-quality spectrum, e.g. significant decrease in signal-to-noise ratio. In the worst case, the neutron brings a permanent defect to the CCD pixel.

In Large Helical Device (LHD), a deuterium experiment was initiated in March 2017 and continued for the following four months under an operational constraint of annual neutron yield limited to 2.1×10^{19} .¹³ Then, the

D-D experiment over four months has been controlled not to exceed the annual regulation value. During the D-D experiment, totally 3.7×10^{18} neutrons have been yielded mainly through a beam-target reaction. The γ -ray energy distribution is simulated for the D-D experiment of LHD.¹⁴ The result indicates that the γ -ray flux is dominant at $E_\gamma \leq 1$ MeV, while the γ -ray energy distributes in a wide range of 0.01-12.0 MeV.

Many CCDs are equipped on vacuum spectrometers working in vacuum ultraviolet (VUV), extreme ultraviolet (EUV) and X-ray ranges. Although these CCDs are located at different toroidal positions and different distances from the plasma center of LHD, a large amount of noise caused by neutrons and γ -rays have been observed in all CCDs during the D-D experiment. An effect of neutrons and γ -rays on the CCD is then examined against the CCD location. In addition, two special shielding boxes made of polyethylene contained 10% boron and lead are used to make a quantitative analysis on the CCD background noise by changing the shielding material.

II. EXPERIMENTAL SET-UP

In LHD, VUV, EUV and X-ray spectrometers are used in vacuum condition by directly connecting to a diagnostic port. The same back-illuminated CCD (Andor DO420-BN and DO920-BN) is used for all the

^{a)}Published as part of the Proceedings of the 22nd Topical Conference on High-Temperature Plasma Diagnostics (HTPD 2018) in San Diego, California, USA.

^{b)}Author to whom correspondence should be addressed:

liu.yang@nifs.ac.jp.

spectrometers reported here. All the CCDs are operated at $-20\text{ }^{\circ}\text{C}$ for reducing thermal noise. The size of the CCD image area is $26.6 \times 6.7\text{ mm}^2$ and the number of pixels is 1024×255 ($26 \times 26\text{ }\mu\text{m}^2/\text{pixel}$). The arrangement of these spectrometers in LHD is shown in Fig. 1. Impurity behavior in LHD plasmas has been routinely measured with an impurity monitor system installed on #10-O port. Several VUV and EUV spectrometers are arranged at a backside square port (size: $30 \times 220\text{ cm}^2$) of the impurity monitor system. A distance from the plasma center ($R_{ax} = 3.60\text{ m}$) of LHD to the CCD is roughly 9.5 m for all the spectrometers at the impurity monitor system. Three 20 cm normal incidence VUV spectrometers named 109LVUV, 106RVUV and 102RVUV mainly monitor the line spectrum from light impurities in the wavelength range of $300\text{-}1050\text{ \AA}$, $1000\text{-}1850\text{ \AA}$ and $1550\text{-}2400\text{ \AA}$, respectively.⁵ Temporal evolutions of the VUV spectrum are observed every 5 ms in a full-binning mode operation of the CCD. In addition, two grazing-incidence EUV spectrometers called EUV_Short⁶ and EUV_Long⁷ mainly monitor the line spectrum from metallic impurities in the wavelength range of $10\text{-}130\text{ \AA}$ and $50\text{-}500\text{ \AA}$, respectively. The spectrum is also sequentially obtained every 5 ms as well as the VUV spectrometer.

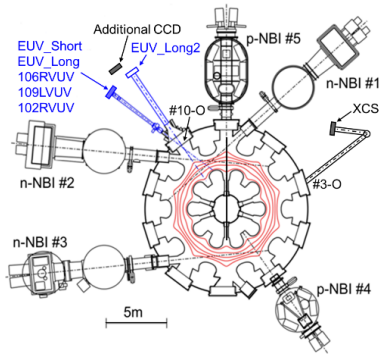


Fig. 1. Arrangement of two EUV spectrometers (EUV_Short and EUV_Long), three VUV spectrometers (106RVUV, 109LVUV and 102RVUV), one Johann-type x-ray crystal spectrometer (XCS) and one additional CCD in LHD.

In the 10-O port, in addition, a space-resolved EUV spectrometer called EUV_Long2⁸ is installed at a backside square port (size: $50 \times 130\text{ cm}^2$) of a cubic vacuum manifold for the spatial distribution measurement of impurity lines emitted in the wavelength range of $50\text{-}550\text{ \AA}$. The CCD is placed at a distance of 9.5 m away from the plasma center of LHD. The short axis of CCD is horizontally placed along the wavelength dispersion. Then, the vertical profile of impurity lines is measured along the long axis of CCD. As the CCD is usually operated in a sub-image mode with five-pixel binning at the long axis and two-pixel binning at the short axis, the CCD signal with an image size of 204×127 channels is recorded every 100 ms .

A Johann-type x-ray crystal spectrometer (XCS)⁹ is installed on #3-O port for monitoring the ion temperature at plasma core by measuring the Doppler broadening of

He-like resonance line of ArXVII. The ion temperature is monitored every 5 ms in a full binning mode of the CCD. The CCD is placed at a distance of 7 m away from the plasma center of LHD.

III. EXPERIMENTAL RESULTS

A. Noise on CCDs of VUV, EUV and X-ray spectrometers during D-D experiment

Three CCD images measured with EUV_Long2 are shown in Figs. 2(a)-2(c), which are taken from hydrogen discharge before the D-D experiment, deuterium discharge during the D-D experiment and hydrogen discharge after the D-D experiment, respectively. In these three discharges, the line-of-sight of EUV_Long2 is fixed to observe the upper-half LHD plasma at horizontally elongated plasma cross section. The horizontal and vertical axes of the CCD image represent the vertical direction of LHD plasma and the wavelength direction, respectively. The CCD sampling time is the same for all three images, i.e., 0.1 s . In Fig. 2(b), the CCD image is taken from NBI discharge with a neutron rate of $S_n = 1.2 \times 10^{15}\text{ n/s}$. Electron temperature and density and NBI port-through power at the CCD image acquisition are $T_e = 3.4\text{ keV}$, $n_e = 2.1 \times 10^{13}\text{ cm}^{-3}$ and $P_{\text{NBI}} = 15.1\text{ MW}$, respectively. Two strong emission lines appeared in the middle of image are from HeII at 303.780 \AA and CIV at 312.420 \AA . Many noises are observed in Fig. 2(b) with white spots which are dominantly caused by neutrons and γ -rays. The total noise count rate, which is defined as the noise count multiplied for all CCD pixels divided by an

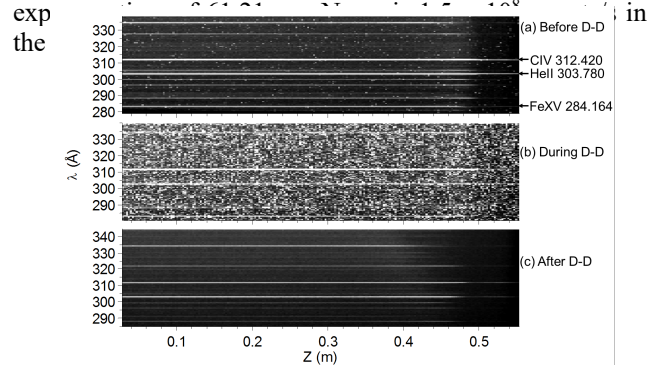


Fig. 2. CCD images taken from EUV_Long2 in (a) NBI discharge before D-D experiment with exposure time of 61.48 ms (#130543: $N_{\text{CCD}} = 0.1 \times 10^8\text{ counts/s}$, $T_e = 1.2\text{ keV}$, $n_e = 3.5 \times 10^{13}\text{ cm}^{-3}$, $P_{\text{NBI}} = 18.7\text{ MW}$), (b) NBI deuterium discharge during D-D experiment with exposure time of 61.21 ms (#138430: $N_{\text{CCD}} = 1.5 \times 10^8\text{ counts/s}$, $S_n = 1.2 \times 10^{15}\text{ n/s}$, $T_e = 3.4\text{ keV}$, $n_e = 2.1 \times 10^{13}\text{ cm}^{-3}$, $P_{\text{NBI}} = 15.1\text{ MW}$) and (c) hydrogen ECH discharge after four month D-D experiment with exposure time of 61.21 ms (#143782: $N_{\text{CCD}} = 0$, $T_e = 1.8\text{ keV}$, $n_e = 4.5 \times 10^{13}\text{ cm}^{-3}$, $P_{\text{ECH}} = 2.5\text{ MW}$).

The CCD image in Figs. 2(a) and 2(c) is taken from hydrogen discharges with NBI ($T_e = 1.2\text{ keV}$, $n_e = 3.5 \times 10^{13}\text{ cm}^{-3}$ and $P_{\text{NBI}} = 18.7\text{ MW}$) before the D-D experiment

and ECH ($T_e = 1.8$ keV, $n_e = 4.5 \times 10^{13}$ cm $^{-3}$ and $P_{ECH} = 2.5$ MW) after the D-D experiment over four months, respectively. It is noted here that the wavelength range in Fig. 2(c) is slightly different from other two figures. Then, the FeXV at 284.164 Å is invisible in Fig. 2(c). The noise detected in these images are extremely weak, while the noise from high-energy neutral particles originated in NBI fast ions¹⁵ can be seen in Fig. 2(a) with small white spots¹⁶. The total noise count from the hydrogen NBI discharge in Fig. 2(a) is $N_{CCD} = 0.1 \times 10^8$ counts/s, while the N_{CCD} from the hydrogen ECH discharge in Fig. 2(c) is basically zero.

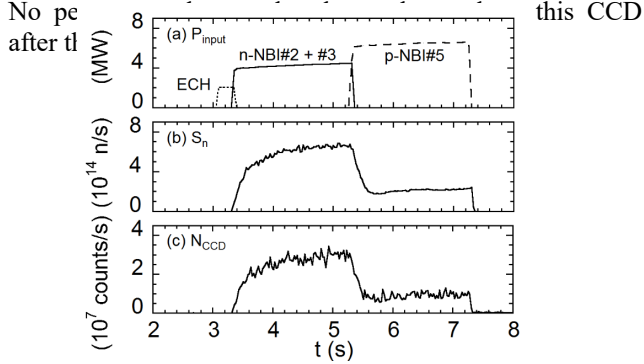


Fig. 3. Time behaviors of (a) input power of NBI and ECH, (b) neutron production rate and (c) total noise count rate in the additional

The noise during the D-D experiment is analyzed for six CCDs, i.e., three for VUV, two for EUV and one for X-ray, which are operated in the full-binning mode for measuring the spectrum as mentioned before. All these CCDs are operated without any shielding during the four-month D-D experiment. Meanwhile, an additional CCD is placed at 10.5 m away from the plasma center of LHD as shown in Fig. 1. It is also operated in the full-binning mode without any shielding. A typical deuterium discharge is shown in Fig. 3. Time behaviors of input power of NBI and ECH, neutron production rate and total noise count rate obtained in the additional CCD are displayed in Figs. 3(a)-3(c), respectively. The CCD noise is analyzed for these seven CCDs by accumulating 200 frames during NBI heating period, e.g., 4.0-5.0 s. For the analysis, a similar plasma parameter phase is chosen for ten deuterium discharges with plasma axis position of $R_{ax} = 3.60$ m. The result is plotted in Fig. 4. The abscissa, L , indicates a distance from the CCD to the plasma center of LHD. In the vertical axis, the total noise count rate in the CCD, N_{CCD} (counts/s), is normalized by the neutron production rate, S_n (neutrons/s), because the neutron production rate is different in these ten deuterium discharges. Therefore, the value of N_{CCD}/S_n should be basically proportional to the number of incident γ -rays and neutrons, if the energy distribution of neutrons and γ -rays is unchanged at these locations where seven CCDs are placed. Then, the result in Fig. 4 seems to indicate that the number of neutrons and/or γ -rays decreases with the distance from the plasma. Anyway, the N_{CCD}/S_n is large

for the XCS CCD which is closely placed to the LHD plasma and is small for the additional CCD denoted “Naked CCD” which is placed at the furthest position from the LHD plasma center. The value of N_{CCD}/S_n differs at least 1

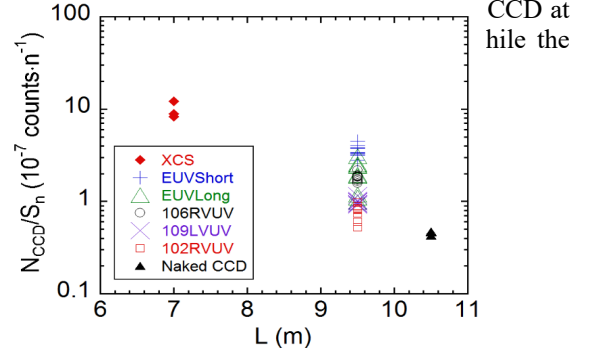


Fig. 4. Total noise count rate normalized by neutron production rate, N_{CCD} / S_n , against distance from CCD to plasma center ($R_{ax} = 3.60$ m) of LHD, L , for XCS, EUVShort, EUVLong, 106RVUV, 109LVUV, 102RVUV and additional CCD without any shielding denoted with Naked CCD.

All CCDs used for the D-D experiment have been carefully checked to find certain damage. However, no permanent defect can be found in the CCD pixel as well as the result in Fig. 2. Only in the XCS CCD it is found that the background noise permanently increases by three times for a few pixels, which never disappear even if the CCD cooling temperature is decreased. Although it is unclear whether the damage on the XCS CCD is caused by the D-D experiment, such a negligibly small damage does not influence the actual use at all.

B. Examination of noise induced by neutron and γ -ray using shielding CCD

The effect of γ -rays and neutrons is then examined in four different ways using the additional CCD, as shown in Fig. 5. At first, the CCD is exposed to neutrons and γ -rays without any shielding (see Fig. 5(a)). Next, the noise is individually examined for the CCD shielded by only 1.5 cm thick lead (see Fig. 5(b)) and by only 10 cm thick polyethylene (see Fig. 5(c)). Finally, the noise is examined for the CCD shielded by both the 1.5 cm thick lead and 10 cm thick polyethylene. External dimensions of lead and polyethylene boxes are 40 cm \times 30 cm \times 30 cm in height and 60 cm \times 50 cm \times 50 cm in height, respectively. The polyethylene plate used here contains 10% boron for an effective capture of thermal neutrons after losing the energy.

As well as Fig. 4, the noise count, N_{CCD}/S_n , is plotted against the total neutron rate in Fig. 6. The relative error for each value is less than 5%. It is found that the shielding effect of lead is clearly more effective than that of polyethylene. In order to estimate the effect of neutrons

and γ -rays individually, the attenuation ratio of γ -ray, I / I_0 , is calculated by the following equation of

$$I / I_0 = e^{-\mu \rho t}, \quad (1)$$

where I_0 and I are the γ -ray flux before and after passing through the shielding material, respectively, and μ , ρ and t are the mass absorption coefficient, the density of shielding material and the thickness, respectively. The mass absorption coefficient of lead and polyethylene for γ -rays is taken from NIST Database.¹⁷ Although the γ -ray energy distribution measurement has been attempted in LHD, the signal is always affected by many noises. Then, the γ -ray energy distribution from the simulation¹⁴ is used for the present analysis. The analysis indicates that the averaged attenuation ratio of γ -rays in lead is 0.1914. The attenuation ratio of fast neutron against 1.5 cm thick lead is calculated to be 0.8383 based on the removal cross section.¹⁸ Here, a shielding efficiency ratio is defined as K / K_0 , where K and K_0 mean the total noise count with and without shielding, respectively. The value of K can be written by

$$K = N_{\gamma} + N_n \quad (2)$$

From Fig. 5, it is determined that the shielding efficiency ratio is 29% for lead, 10% for polyethylene and 10% for lead plus polyethylene.

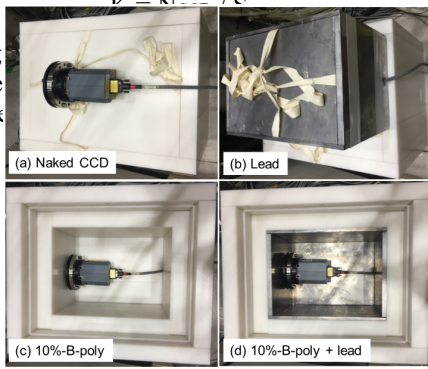


Fig. 5. (a) CCD without shielding, (b) CCD with lead, (c) CCD with polyethylene contained 10% boron and (d) CCD with polyethylene contained 10% boron and lead. External dimensions of lead and polyethylene boxes are 40 cm \times 30 cm \times 30 cm in height with a thickness of 1.5 cm and 60 cm \times 50 cm \times 50 cm in height with a thickness of 10 cm, respectively.

The lead is quite ineffective to reduce the neutron energy due to the large mass and can simply attenuate the γ -ray. In the case of polyethylene with 10% boron, on the other hand, the reaction process with neutrons is a little complicated. The neutron mainly reduces the energy through a collision with the boron and hydrogen, while a low-energy neutron captured by the boron and hydrogen emits a γ -ray with energy of 0.48 MeV and 2.2 MeV, respectively. Meanwhile, a low-energy γ -ray can be partly attenuated by the polyethylene. Here, it is attempted to estimate the effect of γ -rays on the CCD quantitatively based on the present data. If the noise count per γ -ray and

neutron can be defined by $\eta(\gamma)$ and $\eta(n)$, respectively, the shielding efficiency is expressed by

$$K_0 = I_0(\gamma) \times \eta(\gamma) + I_0(n) \times \eta(n), \quad (3)$$

where $I_0(\gamma)$ and $I_0(n)$ are the flux of γ -rays and neutrons, respectively. When the CCD is shielded by lead, the equation is rewritten by

$$K = I(\gamma) \times \eta(\gamma) + I(n) \times \eta(n), \quad (4)$$

where $I(\gamma)$ and $I(n)$ are the flux of γ -rays and neutrons for the CCD shielded by lead. The attenuation of γ -rays is then calculated from the eq. (1) as

$$I(\gamma) = 0.19 \times I_0(\gamma). \quad (5)$$

If the neutron has no collision in the lead, we obtain a relation of

$$I(n) = 0.84 \times I_0(n). \quad (6)$$

The shielding efficiency ratio for lead is already obtained from the experiment as

$$K / K_0 = 0.5749. \quad (7)$$

From the eqs. (3)-(7), thus, the ratio of noise count caused by γ -rays to the total noise count is determined as

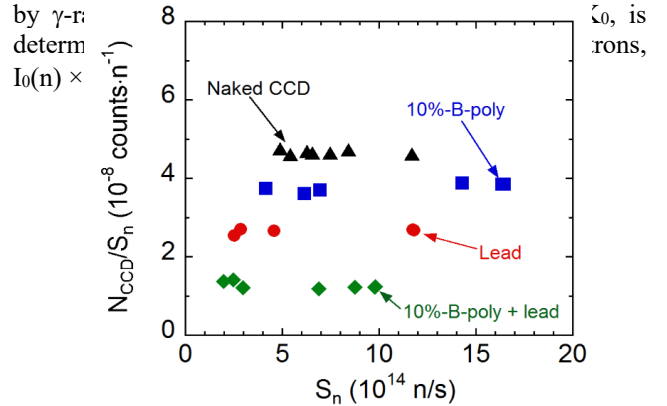


Fig. 6. Total noise count rate normalized by neutron production rate, N_{CCD} / S_n , against neutron production rate, S_n , for CCD without shielding (solid triangles) and shielded with lead (solid circles), polyethylene contained 10% boron (solid squares) and polyethylene plus lead (solid diamonds).

C. Reduction of noise

A lot of noise appears for all CCDs placed in the LHD laboratory during the D-D experiment. A reduction of the noise from the spectrum is attempted by the following method. A raw EUV spectrum at wavelength range of 270-320 Å from a single frame (5 ms exposure time) of the CCD data is shown in Fig. 7(a), which is measured with EUV_Long at $t = 4.5$ s in a deuterium discharge. It is not easy to identify an impurity emission line from the spectrum. When the spectrum is accumulated during $t =$

4.3-4.7 s as shown in Fig. 7(b), the randomly appeared noise can be averaged and a few impurity lines with relatively strong intensity become visible. For the comparison, a single frame spectrum measured at the same wavelength range in a hydrogen discharge is shown in Fig. 7(c). It is clear that both spectra are basically identical. Therefore, if the impurity line intensity is relatively strong, the present signal accumulation method is fairly effective for reducing the noise.

A reduction of the noise is also possible for the profile measurement with the sub-image mode CCD operation. A vertical profile of HeII at wavelength interval of $303.56 \text{ \AA} \leq \lambda \leq 304.03 \text{ \AA}$ measured with EUV_Long2 at $t = 4.5 \text{ s}$ in a deuterium discharge is shown in Fig. 7(d). Many spike noises appear in the vertical profile. Figure 7(e) shows the same profile after removing the spike noise with a simple software programming by directly connecting two nearby channels. The comparison of the HeII profile measured in deuterium discharge and hydrogen discharge is shown in Fig. 7(f).

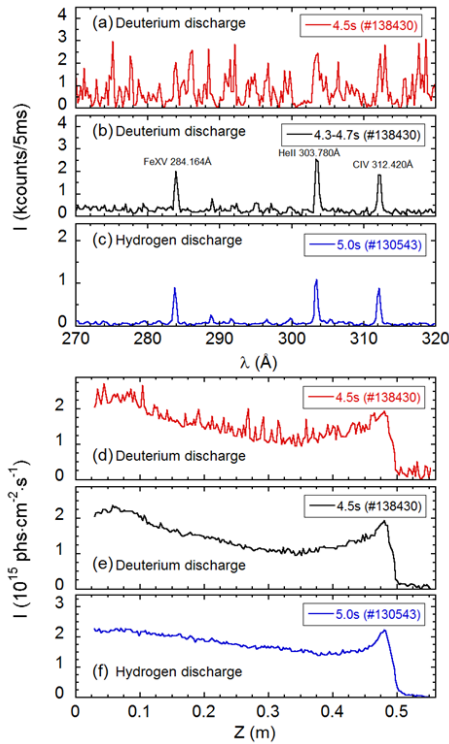


Fig. 7 (a) Raw EUV spectrum from a single CCD frame (5ms exposure) measured with EUV_Long at $t = 4.5 \text{ s}$ in deuterium discharge (#138430), (b) EUV spectrum averaged with 80 CCD frames during 4.3-4.7 s (#138430), (c) raw EUV spectrum from a single CCD frame measured at $t = 5.0 \text{ s}$ in hydrogen discharge (#130543), (d) vertical profile of HeII at 303.780 \AA measured with EUV_Long2 at $t = 4.5 \text{ s}$ in deuterium discharge (#138430), (e) vertical HeII profile with software noise removal modified from (d) and (f) vertical HeII profile measured in hydrogen discharge

IV. SUMMARY

An effect of noise caused by neutrons and γ -rays on CCD is examined in deuterium plasma experiments of LHD. The noise is analyzed for seven CCDs installed on VUV, EUV and X-ray spectrometers which are located at a different distance ($7 \text{ m} \leq L \leq 10.5 \text{ m}$) from the plasma center of LHD. The result indicates that the noise count per neutron decreases with the distance. The noise is also quantitatively examined using a special CCD placed in a shielding box made of 1.5 cm thick lead and 10 cm thick polyethylene containing 10% boron. Analyzing the noise obtained by changing the shielding material, it is found that the neutron contribution to the total CCD noise is smaller than the γ -ray contribution, i.e., 59% for the neutron and 41% for the γ -ray. The radial profile measurement is not significantly affected by the noise because the intensity gradually changes against the radial position. The noise effect becomes more serious in the spectrum measurement. However, the spectrum with random spike noises can be improved, if several CCD frames are accumulated. Finally, we can conclude that the CCD used in the present study has entirely no permanent damage, at least, for the D-D experiment with totally 3.7×10^{18} neutron yields.

V. ACKNOWLEDGMENTS

The authors thank all the members of the LHD experiment group for their cooperation including technical support. The authors also thank Prof. T. Nishitani for his helpful advice. This work was partly carried out under the LHD project financial support (NIFS17ULPP010) and also partly supported by Grant-in-Aid for Scientific Research (B) No. 16H04088.

VI. REFERENCES

- ¹R. Reimer et al., Rev. Sci. Instrum. **84**, 113503 (2013).
- ²K.H. Burrell, D.H. Kaplan, P. Gohil, D.G. Nilson, R.J. Groebner and D.M. Thomas, Rev. Sci. Instrum. **72**, 1 (2001).
- ³L. Zhang et al., Rev. Sci. Instrum. **86**, 123509 (2015).
- ⁴W.H. Ko, H. Lee, D. Seo and M. Kwon, Rev. Sci. Instrum. **81**, 10D740 (2010).
- ⁵T. Oishi, S. Morita, X. Huang, H. Zhang, M. Goto and the LHD Experiment Group, Plasma Fusion Res. **10**, 3402031 (2015).
- ⁶M. B. Chowdhuri, S. Morita and M. Goto, Appl. Opt. **47**, 135-146 (2008).
- ⁷M. B. Chowdhuri, S. Morita and M. Goto, Rev. Sci. Instrum. **78**, 023501 (2007).
- ⁸C. Dong, S. Morita, M. Goto, and H. Zhou, Rev. Sci. Instrum. **81**, 033107 (2010).
- ⁹S. Morita and M. Goto, Rev. Sci. Instrum. **74**, 2375 (2003).
- ¹⁰P.A. Jaanimagi, R. Boni and R.L. Keck, Rev. Sci. Instrum. **72**, 801 (2001).
- ¹¹C. Hagmann et al., Proc. SPIE **8144**, 814408 (2011).
- ¹²A. Huber et al., Fusion Eng. Des. **123**, 669 (2017).
- ¹³M. Osakabe et al., Fusion Sci. Technol. **72**, 199-210 (2017).
- ¹⁴T. Nishitani, K. Ogawa, H. Kawase, N. Pu, T. Ozaki and M. Isobe, Nucl. Sci. Technol., under progress.
- ¹⁵T. Ozaki et al., Rev. Sci. Instrum. **74**, 1878 (2003).
- ¹⁶X. Huang, S. Morita, T. Oishi, M. Goto and C. Dong, Rev. Sci. Instrum. **85**, 043511 (2014).
- ¹⁷J.H. Hubbell and S.M. Seltzer, National Inst. of Standards and Technology-PL, Gaithersburg, MD (United States). Ionizing Radiation Div., 1995.

